

**QTMC**  
**QM Truncated Moments Corrector for**  
***PEACE* on-board moments**

**User Guide v1.0.7**

J. Geach & S. J. Schwartz

*Space Plasma Group, Queen Mary, University of London*

V. Génot

*CESR, Toulouse, France*

March 2005

# Contents

<b>1</b>	<b>QTMC – User guide</b>	<b>2</b>
1.1	Licenses . . . . .	2
1.2	Installation . . . . .	2
1.3	Error codes . . . . .	3
1.4	Batch mode . . . . .	4
1.5	Interactive mode . . . . .	6
1.6	The log file . . . . .	7
1.7	Moment sums & $\Delta\Phi$ . . . . .	7
1.8	Troubleshooting . . . . .	9
1.9	Practical details . . . . .	10
1.9.1	Running QTMC blind . . . . .	10
1.9.2	Scripting & optimization . . . . .	10
<b>2</b>	<b>Spacecraft moments: introduction</b>	<b>11</b>
<b>3</b>	<b>Definitions</b>	<b>13</b>
3.1	Moments of the velocity distribution function . . . . .	13
3.2	Nomenclature . . . . .	14
<b>4</b>	<b>The algorithm</b>	<b>17</b>
4.1	Choice of frame . . . . .	17
4.2	The normalised non-linear system . . . . .	17
4.3	Adding high energy moments . . . . .	18
4.4	Temperature anisotropy estimation . . . . .	19
4.5	Estimation parameters . . . . .	20
<b>5</b>	<b>Calibration</b>	<b>21</b>
5.1	Energy look-up tables . . . . .	21
5.2	Overlap moments separation and sum . . . . .	21
5.3	Gain correction factors . . . . .	22
5.4	Frame transformation . . . . .	23
<b>6</b>	<b>Useful information</b>	<b>25</b>
6.1	<i>PEACE</i> operations history key . . . . .	25
6.2	<i>Cluster</i> spacecraft identifiers, nomenclature and plotting guidelines . . . . .	26

# Chapter 1

## QTMC – User guide

### 1.1 Licenses

*QTMC* falls under the GNU General Public License (GPL), though utilises libraries developed by the South West Research Institute (SwRI), which requires a separate license if the software is built from source. These are contained in the file `LICENSES`, distributed with this software.

### 1.2 Installation

*QTMC* relies on several other pieces of software and libraries to run:

1. *South West Data Display and Analysis System (SDDAS) – Instrument Data File Set (IDFS)*. These libraries handle the promotion and ingestion of spacecraft data – note they do not fall under the GNU General Public License, and if you build the software, then you must sign the associated license.  
<http://www.idfs.org>
2. *Common Data Format (CDF)* is a format which stores data and metadata, and is extremely useful for the storage and manipulation of the corrected moment data. *QTMC* requires some of the *CDF* header files.  
[http://nssdc.gsfc.nasa.gov/cdf/cdf\\_home.html](http://nssdc.gsfc.nasa.gov/cdf/cdf_home.html)
3. *CEF/QFT/CDF* translator *Qtran*. This is not essential, since both the CEF and QFT formats are supported by *QTMC*, however without *Qtran*, no CDF files can be generated. Note that only the executable *Qtran* is needed, and *QTMC* can be built without the *Qtran* source code.  
[http://www.space-plasma.qmul.ac.uk/QSAS/qtran\\_welcome.html](http://www.space-plasma.qmul.ac.uk/QSAS/qtran_welcome.html)
4. If you wish to run the software in interactive mode, you will require the *Qt* libraries. These are distributed with flavours of Linux which support KDE.  
<http://www.trolltech.com/products/qt/>

*QTMC* can run in batch-mode (i.e. invoked with full options from the command line), or in interactive mode (which relies on the *Qt* libraries). The software can be built either with or without *Qt* by using the appropriate Makefile. If *QTMC* is built without *Qt*, then only the batch-mode can be used.

Additionally, there are some underlying libraries distributed with *QTMC* which are borrowed from another software suite, QSAS. You can use those binaries, or rebuild them here: `libqdos.so`, `libqblas.so` and `libqlapack.so`, which reside in the `./lib` directory. These are needed by *QTMC* for the way it handles the data objects and certain underlying mathematical functions. To clean out all binaries and begin, build these libraries by executing the lines:

```
build Makefile_no(w)Qt clean
build Makefile_no(w)Qt qdos
build Makefile_no(w)Qt qblas
build Makefile_no(w)Qt qlapack
which should build the .so or .a files and put them in ./lib.
```

Then, for the non-Qt version, execute the line:

```
build Makefile_noQt
```

This will put the binary executable `QTMC_noQt` in the `./bin` directory.

For the Qt version, execute the line:

```
build Makefile_wQt
```

This will put the binary executable `QTMC` in the `./bin` directory. So far *QTMC* has been successfully built on the *Mandrake 9.x* flavour of Linux.

The *QTMC* binary can be run directly if you add the necessary paths and environments to your shell, e.g., edit your (e.g.) `.tcshrc` file to include:

```
setenv QTMC_HOME /local/path/qtmc
```

and add the *QTMC* `.lib` directory to the `LD_LIBRARY_PATH`:

```
setenv LD_LIBRARY_PATH ${LD_LIBRARY_PATH}:${QTMC_HOME}/lib.
```

You'll also need to add the CDF libraries in the same way. Next, edit the `build` script to point to local locations of various dependencies (described above).

Alternatively, a script to do all this, `qtmc_ui`, is supplied in the *QTMC* bin directory. This script will need to be edited to point to your local installation. Other scripts for command-line operation are also provided, and can be modified to set the necessary environment variables.

### 1.3 Error codes

The main solver routine returns a code referring to the success or failure of the algorithm. A correcting failure is defined as a time when the algorithm failed to converge to a result within the maximum number of iterations allowed (50), or an error related to bad input data: the nature of this failure is described by an integer code. *QTMC* filters out all failures before outputting the final corrected data sequence, however the successful points are categorized by a 'success' code – 0, 6 or 9. They can be described as follows:

- 0 successful solve
- 6 successful solve, but needed to invoke guessing loop
- 9 successful solve, but did not include BOTTOM moments

Code 9 refers to moment sums where the user has specified that the BOTTOM moments (*PEACE* nomenclature will be discussed later) should be used, but the solver has not used them for fear of contamination by photo-electrons. This feature is described fully below in section 1.7. The failed data points are invisible to the user, as the output series will never contain any failed points (though a record will exist if the user has output a log file). The most common form of failure is iteration exhaustion (code 7), though occasionally other errors will cause the solver to fail (e.g. incorrect inputs, corrupt data, etc.) – each code has an associated message which describes what went wrong.

The output file contains the successful codes as a time-series, which can be compared directly with the corrected moments to show regions where, for example, the B moments were not included, or points where the guess loop was needed.

## 1.4 Batch mode

*QTMC* can be executed in batch mode from the command line by providing the following arguments. Bold face type indicate mandatory inputs. Values in ‘[ ]’ represent defaults.

```

-S{start time YYYY-MM-DDZHH:MM:SS.SSS or YYYY-DDDZHH:MM:SS.SSS}
-E{end time YYYY-MM-DDZHH:MM:SS.SSS or YYYY-DDDZHH:MM:SS.SSS}
-M{SC ([1]-4)}{SUM [BL1L2T]}
-C{location of calibration files}
-D{location of output data}
-O{output format [cef]/qft/cdf}
-U{delta Phi [0.0 V]}
-V{manual s/c potential [7.0 V]}
-o{over-ride EFW U_probe_sc yes/[no]}
-l{lower limit of guess loop [-200%]}
-u{upper limit of guess loop [200%]}
-r{resolution of guess loop [1%]}
--reticent {turn off logging}
--clobber {overwrite existing files}
--history {by-pass calculation and print basic command history}

```

The value of ‘manual spacecraft potential’ is used if the EFW (*Electric Fields and Waves*) probe value is unavailable, or if the user requests that the EFW probe value should not be used (over-ride EFW option).

A minimal example of a literal *QTMC* execution could be (arguments have been put on separate lines for clarity):

```

QTMC -S2002-075Z14:00:00.000
      -E2002-075Z15:00:00.000
      -M2BH1H2T
      -C$(QTMC_HOME)/cal

```

```
-D/data/cluster/sc2
```

This command corrects the BH1H2T moment sum from spacecraft 2 over the interval 1400 hrs to 1500 hrs on March 16, 2002. The data is put in some local repository, and the calibration files are retrieved from the *QTMC* distribution `./cal` directory (`QTMC_HOME` should be set as an environment variable). These calibration files were accurate at the time of the last distribution (though could be updated in future). All other options have their default values. A more complicated example could be:

```
QTMC -S2002-075Z14:00:00.000
      -E2002-03-16Z15:00:00.000
      -M2BH1H2T
      -C$(QTMC_HOME)/cal
      -D/data/cluster/sc2
      -U1.5
      -l-1000
      -u1000
      -r100
      -Ocdf
      --clobber
```

This command accesses the same interval as above (but note the time format for `-S` and `-E` is different – this mixing *is* allowed). Here some more options are used:  $\Delta\Phi$  is set to 1.5 Volts and the guessing loop has been extended. Finally, files are output in the CDF format and any existing files of the same name are overwritten (with `--clobber`). Filenames follow a strict convention:

```
TMC_SCN_YYYYDDDDHHMM_YYYYDDDDHHMM_SUM.cdf(qft)
```

Where ‘TMC’ indicates that these are corrected truncated moments; ‘SCN’ refers to the spacecraft number (N ranges from 1 to 4); the first ‘YYYY...’ block indicates the start of the data interval; and the second block the end of the interval. Finally ‘SUM’ could be any one of L1L2, H1H2, BL1L2, BH1H2, L1L2T, H1H2T, BL1L2T or BH1H2T – depending on the requested sum. The extension follows from the user’s output format request. If `clobber` is off, then files of the same name will have an ‘A’ appended to the filename:

```
TMC_SCN_YYYYDDDDHHMM_YYYYDDDDHHMM_SUMA.cdf(qft)
```

Subsequent files will have another ‘A’ and so on.

If the `--history` is requested, then promotion of data will still occur, but the correction will be by-passed and basic *PEACE* operational data will be printed to the console. The energy-scan of both LEEA and HEEA are output (in telemetered units) and the user is informed if there are B, T or overlap moments present. This information is generated for the start and end of the interval requested, and for any scan changes within that interval. For example, the following command:

```
QTMC -S2002-01-03Z04:00:00.000 -E2002-01-03Z06:00:00.000 -M1 --history
gives the following output:
```

```
2002-01-03 03:59:58.180      0      1      0      67 - 16      67 - 16
2002-01-03 05:59:56.735      0      1      0      67 - 16      67 - 16
```

The columns are: time, B moments present? (Boolean), overlap (L1L2 or H1H2) moments present?, T moments present?, HEEA scan (upper - lower), LEEA scan (upper - lower) (both in telemetered units, or bin numbers). Note that the arguments contain a minimal subset of options described previously, without some of the mandatory options. This is somewhat of a hack, since for the command history only a data interval and spacecraft number is required: no real calculation is performed, and no output file is generated. Even the sum request (e.g. `-M1BL1L2T`) can be omitted, since it is inferred from the energy scan. It doesn't hurt to include the other options though. If *PEACE* data cannot be found, then a message will be printed to console.

Perhaps the most powerful application of *QTMC* is via a custom written script which can loop over hours, days, weeks or months worth of data. Such jobs can be left to run unaided by the user to provide an almost automated correcting facility. *QTMC* comes with both a simple *Perl* and *Csh* script to whet the user's appetite. They can be found in the `./bin` directory.

## 1.5 Interactive mode

If only the switches `-C` and `-D` are provided, then *QTMC* will execute in GUI mode, providing a simple graphical interface which allows the user to control all the settings and options described above. Figure 1.1 is an image of the interface.

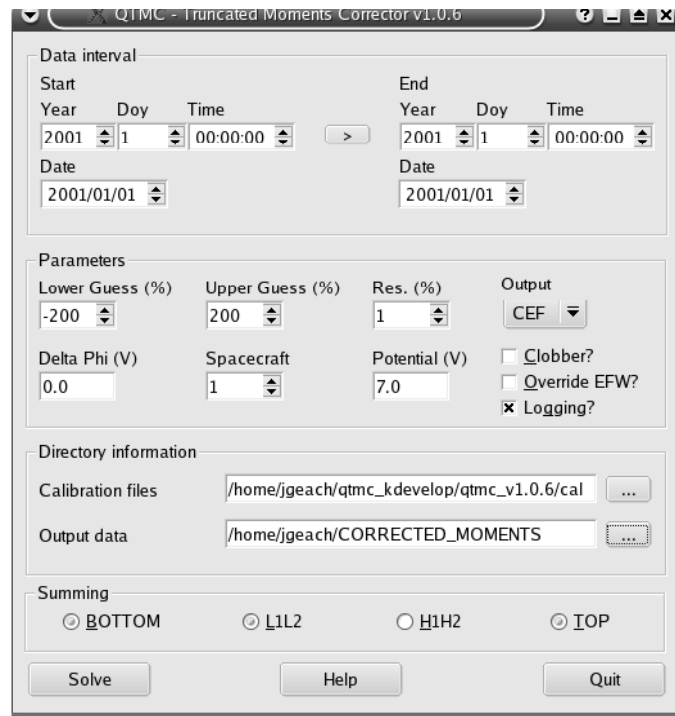


Figure 1.1: *QTMC* user interface.

## 1.6 The log file

If the user has not specified that *QTMC* is executed in reticent mode, then a log will be written containing all the essential data describing each point which was attempted to correct. The log file has the same name structure as the data file and has the extension `.log`. It contains the following information:

- Point index and time tag
- Error code and message
- Raw moments (i.e. input moments) – note velocity vector is converted to GSE frame
- Corrected moments
- Diagnostic factors (discussed later)
- Energy range lookup values  $E_{L,U}$
- Sensor mode (SINGLE or DOUBLE)
- Gain correction factors used for B, overlap and T moments
- Supplementary data: EFW potential, FGM b-vector, AUX latitude and longitude
- Guess window parameters
- Messages to say if B or T were present/used

The log file is very useful if correcting moments for an ‘unknown’ period, as it contains data which is vital to the calculation, but not output in the final file. Even if logging is off, a small summary containing useful information is printed to the console at the end of the calculation.

## 1.7 Moment sums & $\Delta\Phi$

We can construct any of the following sums: L1L2, H1H2, BL1L2, BH1H2, L1L2T, H1H2T, BL1L2T and BH1H2T. Note we cannot mix L1L2 and H1H2 to form for example L1H2. If *PEACE* is operating in single sensor mode (i.e. all the moments are in TOP or BOTTOM), then the software will detect it and proceed as required (and report to the log file). It is possible to request for example the sum BL1L2T, when in fact there are no B or T moments (i.e. sensors are in complete overlap). Again, the software will check for this and behave accordingly – information about the sum is recorded in the log file (note - the filename structure will retain the requested sum).

We have devised a method to filter out the effects of contamination from photo-electrons where we make a choice not to include the B moments (if present) if the lower energy cut-off is within a certain threshold limit of the spacecraft potential (see Figure 1.2). This has the effect of not including the low energy (e.g.  $< 10$  eV) electrons at the expense of raising  $E_L$  and eliminating a wider portion of phase-space. If the solver makes this decision, then an error code will be returned indicating that the B moments were not included for that record. By plotting or inspecting the sequence of error codes, the user can investigate regions of data where filtering has taken place. The threshold limit we call  $\Delta\Phi$ , and is a user-controllable parameter. Raising  $\Delta\Phi$  will result in more instances where B moments are discarded, and lowering it will result in fewer instances where B moments are discarded.

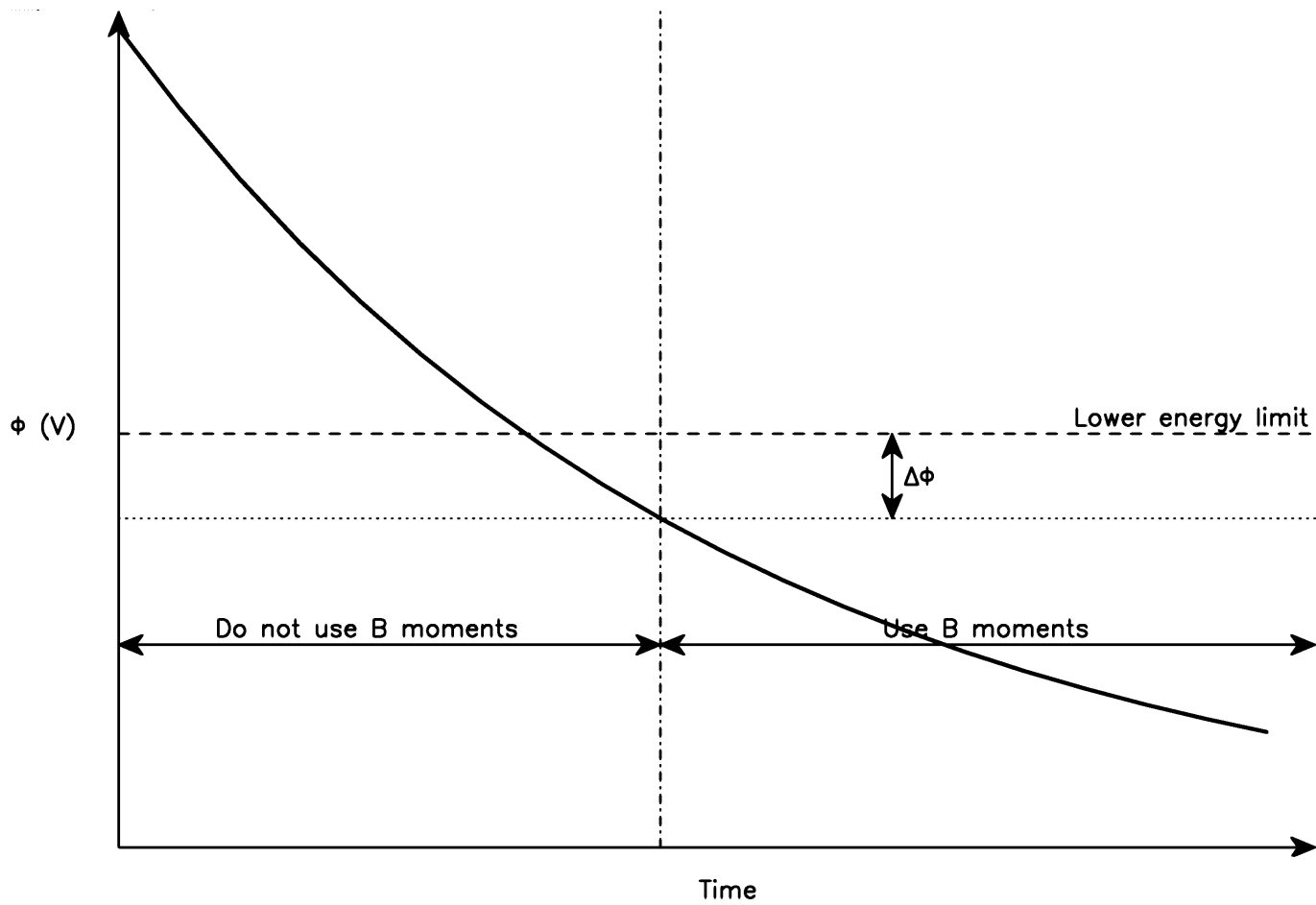


Figure 1.2: Diagram demonstrating B moment filtering. The spacecraft potential is varying with time (thick line). The lower energy level can be considered constant (in reality it doesn't have to be). A threshold is set ( $\Delta\Phi$ ) such that if the potential of the spacecraft breaches it, then the B moments are not used. It can be seen that increasing ( $\Delta\Phi$ ) will result in more stringent filtering of the B moments.

Its default setting is zero Volts; that is, excluding B moments for times when the spacecraft potential exceeds the lower energy cut-off.

## 1.8 Troubleshooting

<i>Symptom</i>	<i>Cause/Solution</i>
Installation difficulties	Check you have all the required libraries, etc. and that you have edited the <code>build</code> script to point to your local versions. If you don't have <i>Qt</i> , then build with the <code>no-Qt</code> option. If you have not done so already, try to rebuild the <code>libqlapack</code> , <code>libqblas</code> and <code>libqdos</code> sharable libraries.
Cannot get data sequence	No data within time requested, check command log to see what <i>PEACE</i> 's operating mode was. Note, if there is no EFW data, a manual value of potential can be used; also if there is no FGM data, the anisotropy will not be estimated.
Error separating overlap moments	Errant time-tag within series. Although <i>QTMC</i> filters out misplaced time-tags, it is possible that the occasional one will slip through. Try adjusting the data interval slightly.
Main calculation failure	Exception encountered while in the main loop.
Input error	Invalid input field. Common problems are: mixing of L1L2 and H1H2 moments, and Invalid time entries. Note that the end time must be at least 10 seconds ahead of the start time. Times must be entered in the correct ISO format (see above).
Promotion error	Data is accessed via an external server. If the server is down/inaccessable, then data will not be retrieved, and the user will be warned. Alternatively if there is insufficient space left on the disk, promotion will fail.
Join error	<i>See 'Error separating overlap moments'</i>
Nil sequence	For whatever reason, a data sequence with no entries has been created. This will inevitably cause a problem somewhere in the calculation, so an error is returned when this situation arises.
Failed to create output sequence	Insufficient memory to accomodate output series.
File read/write error	Check you have the necessary permissions to read the

calibration files and write data to the disk.

No anisotropy?	If the FGM data is not available, then no anisotropy estimation will be made. The other outputs are unaffected. A message indicating that no anisotropy will be output is printed to the console.
Potential not what I was expecting!	Again, if the EFW data is unavailable, then <i>QTMC</i> will use a default value (which you can control, but initially set to 7 V). This information is again conveyed by the console.

## 1.9 Practical details

### 1.9.1 Running QTMC blind

Often, the user will know that there is on-board coverage of a certain interval before attempting to correct the moments. Conversely, it is possible to run the software ‘blind’ – i.e. to attempt to correct an interval about which you have no prior knowledge of coverage. If there are any moments within the interval requested (and there is associated data such as AUX (attitude) data), then those moments will be corrected. The start and end times of these moments may represent only a short portion of the input start and end times (and this will be conveyed in the summary at the end of the calculation), however the filename will contain the input times as part of its construction. This could be slightly misleading to the unwary, so it is advisable to consult the command history of *PEACE* (or use the `--history` option). Note that if the EFW and/or FGM data is not found, then the correction will still proceed, but for the potential a constant user-defined value (default 7 V) will be used and/or no anisotropy will be estimated. Again, this is conveyed to the user on the console.

### 1.9.2 Scripting & optimization

Instead of running the corrector blind, you may wish to try to access and correct all the moments over a long duration (you would construct a script to accomplish this). Now the optimal data interval length becomes important, since the user must consider the managability of file sizes, and the possibility of reducing losses of data if the calculation fails during a particularly long run. Probably the maximum/optimal data interval (from existing user experience) is about 4 hours. This way, output files are easily managable, and each correction pass is relatively fast. Another way to speed up calculation on long batch operations is to make the guess loop step resolution quite coarse, and, erring on the side of caution, make the loop quite large (say `-l-1000, -u1000, -r100`).

Batch mode scripts can be written in your preferred language, for example *Csh* or *Perl*. The simple looping and arithmetic capabilities of scripting languages allow the user to construct powerful automated correcting facilities. Note that *QTMC* prints information to the console for (a) promotion of data, (b) progress of the calculation and (c) summary of calculation. In batch mode you should redirect this output to a file (say called `console.log`) and watch its progress with `tail`. For example, to execute the script `'qtmcbatch'`:

```
@> chmod +x qtmcbatch           Make the script executable (could also use chmod 755)
@> qtmcbatch > console.log &    Run script in background and redirect output to log file
@> tail -f console.log          Watch progress of console.log. Kill with Ctrl+C
```

## Chapter 2

# Spacecraft moments: introduction

*Chapters 2–4 are adapted from Geach et al. (2004)*

The space physicist – interested in the moments of the electron distribution around the Earth – must strike a balance between the advantages and disadvantages of on-board calculations of the moments. Under most circumstances there is insufficient telemetry to transmit samples from the distribution function itself at a high time resolution, but there is ample bandwidth to transmit the moments, which encode basic information about the distribution in just a few numbers.

Moments calculated on-board spacecraft typically over- or under-estimate the values of the ‘true’ moments, because they convolve effects caused by the presence of a potential (from the spacecraft itself) and lower and upper energy truncation imposed by the detector. Furthermore, the plasma environment determines the formation of photo- and secondary electrons, which can return to the spacecraft and enter the detector, therefore contaminating the measured moments. Conversely, full-distribution telemetry can be treated on the ground, using more sophisticated computation than is available on the spacecraft.

Generation of spacecraft potential is determined by the balance of the currents flowing away from the craft carried by liberated electrons, and the incident electrons and ions from the ambient plasma. The value of the potential is therefore determined by the plasma environment, specifically the density and temperature (Pedersen (1995), Escoubet et al (1997)). Attempts have been made to dynamically control the potential, such as *ASPOC* (Active Spacecraft POtential Control) on three of the *Cluster* spacecraft (Riedler et al (1997)), which aims to stabilise the potential by emitting a positive (indium) ion beam. Devices such as *ASPOC* can limit the build up of potential (which can reach values of 70 V) to just a few Volts (Schmidt et al (1995)), and in general aim to constrain the potential to less than 10 V (Torkar et al (2001)). While the charging of the spacecraft can be limited, no real detector is free from the constraints of a finite energy range and calibration defects, the latter of which are very difficult to correct after convolution by the on-board calculation. All on-board calculated moments must therefore be treated with caution.

Song et al (1997) present the concept of a perfect plasma detector, which is free from calibration defects, for which the uncertainties in the on-board moments are solely caused by the spacecraft potential, a truncated energy range and the presence of secondary and photo-electrons. Those authors indicate that in the case of electrons, the lower energy cut-off should be calculated as the detector’s nominal lower energy limit minus the spacecraft potential, although they present results for a null potential. Génot and Schwartz (2004, hereafter GS) further this idea of a perfect detector and present a method to disentangle the effects of potential and energy range truncation using a non-linear numerical

routine (though it is important to note that it is not possible to correct for the effects of contamination of secondary electrons - for a discussion on this topic see Szita et al (2001)). GS demonstrate that the measured moments can be expressed as functions of the true moments and the spacecraft potential, where the true moments are those which would be measured by a perfect detector. We implement the technique proposed by GS such that, given a set of measured moments and knowledge of the spacecraft potential and detector limits, the true moments can be recovered; we call these the corrected moments.

The magnitude of the difference between the on-board and corrected moments is a function of both environment and potential. GS show that the solar wind is a region where the moments are seriously affected. For a potential ranging from zero to 10 Volts, the density can be under-estimated by 60% for low potentials to over-estimation of 75% for high potentials. In general the other moments are over-estimated. Those authors make the interesting point that there exists a critical potential for which the on-board density moment equals the corrected one (see GS and Salem et al (2001)), though no such regime exist for the other moments for typical plasma environments. In other regions such as the magnetosheath and magnetosphere, the moments are less severely compromised as in the solar wind, but the effects there are by no means negligible, with up to a 40% under-estimation of the density in the magnetosheath and 10% in the magnetosphere during nominal operating conditions. Fundamentally the presence of a potential affects the width of the distribution function, such that for a naturally broad (i.e. hot) distribution, the extra broadening caused by spacecraft effects is slight; the opposite is true for cool distributions.

A *PEACE (Plasma Electron and Current Experiment)* instrument is flying on each of the four *Cluster* spacecraft, each one capable of measuring the three dimensional velocity distribution of electrons in a range from 1 eV to 25 keV. The energy range is divided into 88 levels - in general the lower energies measured by the LEEA sensor head, and the higher energies by the HEEA sensor head, mounted on the opposite side of the spacecraft. Every half-spin (about 2 seconds), *PEACE* calculates moments of the electron distribution. Under normal-mode telemetry, these data are transmitted to the ground, together with pitch angle distributions and a low energy distribution. Under burst-mode, 3-dimensional distribution data can be transmitted.

Encoded into the moments are quantities related to the physical characteristics of the ambient plasma such as density, temperature and velocity. The telemetered moments are perturbed by the spacecraft potential, and this must be corrected before the Maxwellian values can be inferred. *QTM* performs this correction, and also compensates for unsampled energy ranges and photoelectron contamination.

# Chapter 3

## Definitions

### 3.1 Moments of the velocity distribution function

The  $n^{\text{th}}$  moment of a distribution  $f(\mathbf{v})$  is defined as:

$$\mathbf{M}_n = \int f(\mathbf{v}) \mathbf{v}^n d^3v \quad (3.1)$$

Certain combinations of the moments from an electron velocity distribution have a familiar physical interpretation:

$$N = M_0 \quad (3.2)$$

$$N\mathbf{V} = \mathbf{M}_1 \quad (3.3)$$

$$\mathbf{P} = m_e \mathbf{M}_2 \quad (3.4)$$

$$\mathbf{p} = \mathbf{P} - m_e \mathbf{M}_1 \mathbf{V} \quad (3.5)$$

where  $N$  is the density,  $\mathbf{V}$  the bulk velocity vector,  $\mathbf{P}$  the stress tensor and  $\mathbf{p}$  the pressure tensor. We assume that in free space (i.e. far away from the spacecraft where there are no effects from the potential), the distribution has a Maxwellian shape at temperature  $T$ , and drifts with some velocity  $\mathbf{V}$ :

$$f(\mathbf{v}) = N \left( \frac{m_e}{2\pi kT} \right)^{3/2} \exp \left( -\frac{m_e}{2kT} |\mathbf{v} - \mathbf{V}|^2 \right) \quad (3.6)$$

Integration over all solid angles and energies yields the number density  $N$ . It is easy to see therefore that in general for a finite integration range  $v_l < |\mathbf{v}| < v_u$ , as used in real detectors,  $N$  will be underestimated. Note that the amount the on-board moments are under- or over-estimated is also a function of spacecraft potential (see GS), such that for large potentials the density is over-estimated.

Near the spacecraft the energy conservation of an electron can be expressed:

$$v_m^2 = v^2 - \mathcal{E} \quad (3.7)$$

where  $v$  is the electron velocity in free space (hereafter a subscript ' $m$ ' denotes a parameter as measured by the spacecraft and ' $c$ ' denotes output from the solver. ' $sc$ ' is a value inherent to the spacecraft, such as potential) and  $\mathcal{E}$  corresponds to the free space energy of an electron which arrives at the detector with zero energy:

$$\mathcal{E} = -\frac{2e\Phi_{sc}}{m_e}. \quad (3.8)$$

$\mathcal{E}$  is negative for most of the plasma environments in space, since typically the spacecraft potential  $\Phi_{sc} > 0$  due to the escape of photo-electrons. Liouville's theorem tells us that the distribution function is constant along a phase space trajectory

$$f(v_m, \theta_m, \phi_m) = f(v, \theta, \phi). \quad (3.9)$$

GS make the scalar approximation: namely that only the magnitude of the velocity is affected by the potential (i.e.  $\theta_m = \theta$  and  $\phi_m = \phi$ ). Under this assumption the angular dependence in the moment integrations can be performed analytically, thus reducing the problem to one dimension. By changing the integration element  $v_m dv_m = v dv$  from equation 3.7, the measured moments can be written in terms of  $v$  and  $\mathcal{E}$ . The integration limits are related to the detector cut-offs  $v_{l,u}$  by

$$v_{L,U} = \sqrt{v_{l,u}^2 + \mathcal{E}}. \quad (3.10)$$

In the case of  $v_l^2 + \mathcal{E} < 0$  where the potential reaches a value greater than the lower energy cut-off, we set  $v_L = 0$ . Figure 3.1 is a schematic representation of the measured part of the distribution compared to the corrected part and the underlying (assumed) Maxwellian distribution.

## 3.2 Nomenclature

The *Cluster PEACE* experiment is made up of two sensor heads called LEEA and HEEA (Low and High Energy Electrostatic Analysers), mounted on opposite sides of each of the four *Cluster* spacecraft (Johnstone et al (1997)). Generally LEEA scans the lower energy range and HEEA the upper range, together covering electrons with  $0.7 \text{ eV} < E < 26 \text{ keV}$ . Over the duration of a spin ( $\sim 4 \text{ s}$ ), LEEA and HEEA cover  $4\pi$  steradians of velocity space.

The moment sums can be thought of as combinations of the low energy moments (the B (BOTTOM) moments,  $E \sim 10 \text{ eV}$ ), the high energy moments (the T (TOP) moments,  $E \gtrsim 2 \text{ keV}$ ), and the moments from where the energy scan of LEEA and HEEA overlap (which we call L1L2 and H1H2 respectively) as sketched in Figure 3.2. These separate pieces are telemetered to the ground, where we can construct moment sums covering the entire energy range by summing B, L1L2/H1H2 and T moments. The 'measured' moments (subscript 'm') are the raw sum of, for example B+overlap+T moments, which have not been corrected.

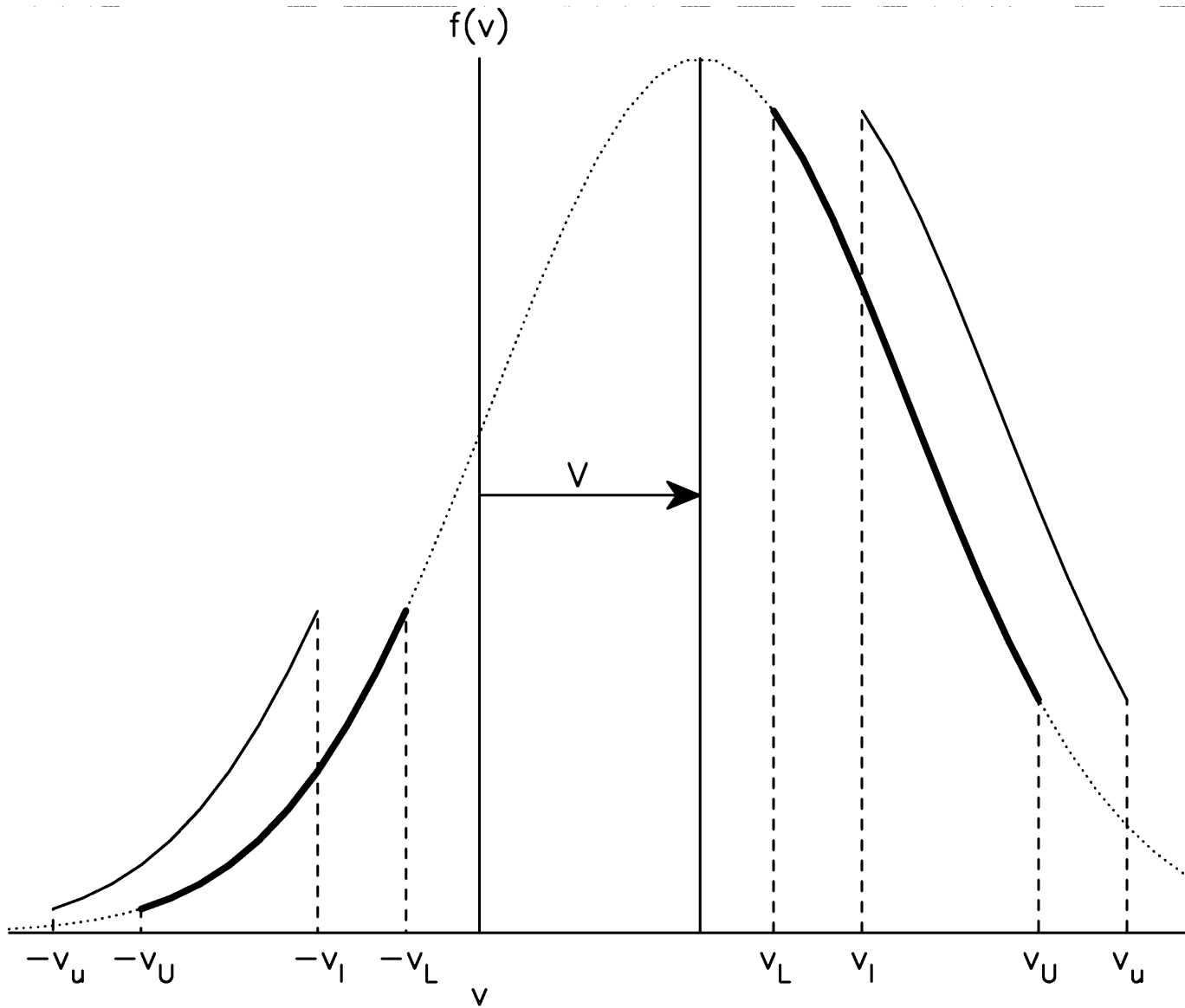


Figure 3.1: Schematic showing the effect of a positive spacecraft potential on an idealised drifting Maxwellian electron distribution (dotted curve). On-board calculated moments are integrals under the shifted segments (solid grey) which can be written, with the help of Liouville's Theorem, in terms of the idealised distribution. Inverting this then yields the Maxwellian parameters.

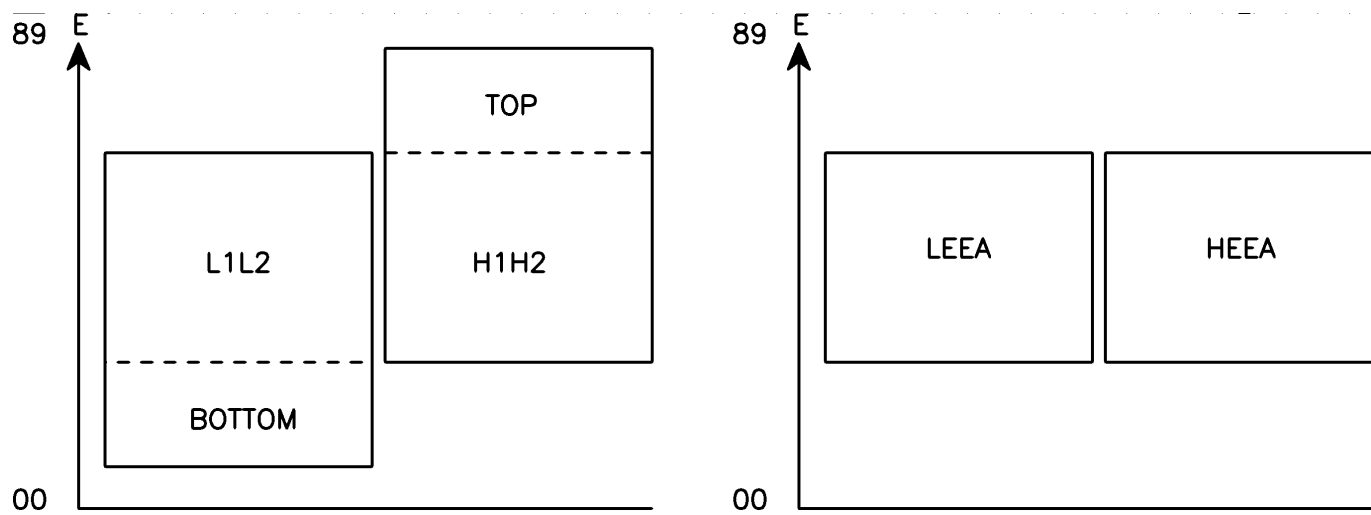


Figure 3.2: Schematic representation of the *PEACE* sensor coverage. The two sensor heads HEEA and LEEA are split into an energy range which is divided into 88 bins. The sensor coverages can overlap by some amount (left), leaving a low energy portion (BOTTOM) and a high energy portion (TOP). The sensors can be made to overlap completely (right) leaving no BOTTOM or TOP moments.

# Chapter 4

## The algorithm

### 4.1 Choice of frame

Our choice of calculation frame simplifies greatly the numerical technique. We transform the spacecraft measurement frame via a rotation  $\mathcal{R}$  which aligns the  $z$  axis with the measured velocity  $\mathbf{V}_m$  such that  $\mathbf{V}_m = (0, 0, |\mathbf{V}_m|)$ . The scalar quantity  $N_m$  remains the same, as does the trace of the pressure tensor. The transformed quantities can be directly inferred from the measured values, so the details of the rotation matrix do not need to be known. As only the magnitude of the velocity is needed, we can use the measured direction of the velocity to recover the corrected velocity vector from the speed derived in our calculation.

The algorithm converges to a solution by improving on a set of initial guesses. The values of initial guess we use were derived from a series of tests in which, given a set of Maxwellian parameters, we simulated measured moments given a range of  $\Phi_{sc}$  and energy cut-offs. We ran our algorithm on these inputs to recover the initial underlying Maxwellian values. The initial guesses were then chosen to be the average values for which the algorithm converged successfully for a range of parameter space which represents typical plasma environments encountered by spacecraft.

### 4.2 The normalised non-linear system

We normalise the unknown moments in terms of the measured ones as:

$$V'_e = \frac{|\mathbf{V}_e|}{V_m} \quad (4.1)$$

$$V'_{Te} = \frac{V_{Te}}{V_{Tm}} \quad (4.2)$$

$$\eta = \frac{1}{\sqrt{\pi}} \frac{N_e/N_m}{V'_e V'_{Te}}. \quad (4.3)$$

Where  $V_{Te}$  is the thermal speed, from which the temperature can be inferred:

$$T_e = \frac{m_e V_{Te}^2}{2k} \quad (4.4)$$

The inputs to the solver are the normalised quantities

$$\zeta_{sc} = \frac{V_m}{V_{Tm}} \quad (4.5)$$

$$\epsilon_{sc} = \frac{\mathcal{E}}{V_{Tm}^2} \quad (4.6)$$

$$V_{L,U} = \frac{v_{L,U}}{V_{Tm}} \quad (4.7)$$

For the inputs  $v_L = 0$ ,  $v_U = \infty$ ,  $\mathcal{E} = 0$ , the exact solution yields unity for equations 4.5 & 4.6 and  $1/\sqrt{\pi}$  for equation 4.7.

The set of non-linear equations which must be inverted are:

$$g_1(N_e, V_e, T_e) - N_m = 0 \quad (4.8)$$

$$g_2(N_e, V_e, T_e) - N_m V_m = 0 \quad (4.9)$$

$$g_3(N_e, V_e, T_e) - 3N_m k T_m - m_e N_m V_m^2 = 0 \quad (4.10)$$

That is, the measured moments are functions of the real moments. We recast to a normalised system such that we wish to find the triplet  $(\eta, V'_e, V'_{Te})$ , given the normalised inputs  $(\zeta_{sc}, \epsilon_{sc}, V_{L,U})$ . The equations to be solved are

$$1 - \frac{\eta}{\zeta_{sc}} \int_{V_L}^{V_U} \sqrt{V^2 - \epsilon_{sc}} (E^- - E^+) dV = 0 \quad (4.11)$$

$$\zeta_{sc}^2 - \eta \int_{V_L}^{V_U} (V^2 - \epsilon_{sc}) \left[ E^- + E^+ - \frac{V_{Te}'^2 (E^- - E^+)}{2V V_e' \zeta_{sc}} \right] dV = 0 \quad (4.12)$$

$$\frac{3}{2} + \zeta_{sc}^2 - \frac{\eta}{\zeta_{sc}} \int_{V_L}^{V_U} (V^2 - \epsilon_{sc})^{3/2} \times (E^- - E^+) dV = 0 \quad (4.13)$$

where

$$E^\pm = \exp \left[ - \left( \frac{V \pm V_e' \zeta_{sc}}{V_{Te}'} \right)^2 \right] \quad (4.14)$$

### 4.3 Adding high energy moments

In practice, we restrict the inversion of (4.8–4.10) to moment sums which exclude the TOP moments of *PEACE*. This improves the numerical accuracy and speed of the algorithm, since high energy moments do not require correcting as the presence of a finite spacecraft potential has negligible effect. These moments (described by the TOP moments in the case of *PEACE*) are incorporated into the overall sum in the following way.

Given the measured onboard moments for  $v < v_u$ , that is,  $(N_m, (NV)_m, \mathbf{P}_m)$ , we use our correcting algorithm to yield the characterising features  $(N_c, V_c, T_c)$  of the Maxwellian distribution  $f(v)$  (equation 3.6). The direction of the velocity is identical to the measured velocity direction by virtue of the scalar approximation. We then perform three 1d integrations on the system  $g_{1,2,3}$  over the truncated range  $0 \leq v \leq v_u$  with a null spacecraft potential to restore the corrected moments into the truncated-corrected form  $(N_{tc}, (NV)_{tc}, \text{Tr}(\mathbf{P}_{tc}))$ :

$$N_{tc} = g_1 [N_c, V_c, T_c, \Phi_{sc} = 0]_{v_L=0}^{v_U=v_u} \quad (4.15)$$

$$(NV)_{tc} = g_2 [N_c, V_c, T_c, \Phi_{sc} = 0]_{v_L=0}^{v_U=v_u} \quad (4.16)$$

$$\text{Tr}(\mathbf{P}_{tc}) = g_3 [N_c, V_c, T_c, \Phi_{sc} = 0]_{v_L=0}^{v_U=v_u} \quad (4.17)$$

where

$$\text{Tr}(\mathbf{P}_{tc}) = 3p_{tc} + 2m_e(NV)_{tc}V_c - m_eN_{tc}V_c^2 \quad (4.18)$$

The direction of  $(NV)_{tc}$  is restored by the measured velocity direction, and the corrected stress tensor is reconstructed into a velocity aligned frame thus:

$$\mathbf{P}_{tc} = p_{tc}\mathbf{I} + m_eN_{tc}(2V_{tc}V_c - V_c^2)\hat{\mathbf{V}}_m\hat{\mathbf{V}}_m \quad (4.19)$$

From here the TOP moments, assumed to reflect the integrals of  $f(v)$  from  $v_u \rightarrow \infty$ , can be added to the truncated-corrected moments yield the final corrected moments:

$$N_f = N_{tc} + N_T \quad (4.20)$$

$$(NV)_f = (NV)_{tc} + (NV)_T \quad (4.21)$$

$$\mathbf{P}_f = \mathbf{P}_{tc} + \mathbf{P}_T \quad (4.22)$$

#### 4.4 Temperature anisotropy estimation

The simplification of the method proposed in GS and implemented here lies in the reduction to a 1d integration, made possible through the use of the scalar approximation and an isotropic distribution. However we can attempt to estimate the anisotropy – i.e. the random velocities parallel and perpendicular to the magnetic field – and interpret the result as two temperature components  $T_{\parallel}$  and  $T_{\perp}$ . Here we describe the estimation.

The  $ij^{\text{th}}$  element of the measured pressure tensor  $\mathbf{p}_m$  can be expressed

$$p_{m_{ij}} = P_{m_{ij}} - m_e(NV)_{mi}V_{mj} \quad (4.23)$$

which can be decomposed in terms of the unit magnetic field vector  $\mathbf{b}$  in the case of a gyrotropic distribution:

$$p_{m_{ij}} = p_{m_{\parallel}}b_i b_j + p_{m_{\perp}}(\delta_{ij} - b_i b_j). \quad (4.24)$$

The trace of  $\mathbf{p}_m$  is then

$$\text{Tr}(\mathbf{p}_m) = p_{m_{\parallel}} + 2p_{m_{\perp}}. \quad (4.25)$$

Finally the measured anisotropy  $A_m$  is found as

$$A_m = \frac{p_{m_{\perp}}}{p_{m_{\parallel}}} = \frac{\text{Tr}(\mathbf{p}_m) - p_{m_{\parallel}}}{2p_{m_{\parallel}}}. \quad (4.26)$$

We make the assumption that this measured anisotropy is an approximation to the underlying anisotropy and so we can partition the corrected temperature  $T_f$  according to:

$$3T_f = T_{f_{\parallel}} + 2T_{f_{\perp}} \quad (4.27)$$

with

$$\frac{T_{f_{\perp}}}{T_{f_{\parallel}}} \equiv A = A_m \quad (4.28)$$

As a check we rotate  $\mathbf{p}_m$  into a field-aligned frame such that:

$$\begin{bmatrix} p_{m00} & p_{m01} & p_{m02} \\ p_{m10} & p_{m11} & p_{m12} \\ p_{m20} & p_{m21} & p_{m22} \end{bmatrix} \rightarrow \begin{bmatrix} p_{m\parallel} & 0 & 0 \\ 0 & p_{m\perp 1} & 0 \\ 0 & 0 & p_{m\perp 2} \end{bmatrix}$$

In practice the off-diagonal terms are not identically zero and we use the ratio of these to the diagonal terms as an error check. Additionally  $p_{m\perp 1} \neq p_{m\perp 2}$  provides a second check.

## 4.5 Estimation parameters

We calculate three estimation parameters which describe how much the measured on-board moments were over- or under-estimated:

$$r_N = \frac{N_m - N_f}{N_f} \quad (4.29)$$

$$r_V = \frac{V_m - |\mathbf{V}_f|}{|\mathbf{V}_f|} \quad (4.30)$$

$$r_T = \frac{\text{Tr}(\mathbf{p}_m)/3N_mk - T_f}{T_f} \quad (4.31)$$

$$I_e = \sqrt{r_N^2 + r_V^2 + r_T^2}. \quad (4.32)$$

These parameters trace the effect that various environments have on the measured moments. A more general estimation parameter  $I_e$  is yielded by the Pythagorean combination of the three parameters above. Generally  $I_e < 1$  (that is,  $< 60\%$  correction on all moments). As mentioned above, the amplitude of the over- or under-estimation is determined by environment, however their general behaviour is also a function of spacecraft potential (which itself is somewhat influenced by the characteristics of the ambient plasma). GS describe how the estimation parameters vary for a range of potentials in three plasma environments: the solar wind, magnetosphere and magnetosheath. Those authors conclude that the moments are affected worst in the solar wind, where  $I_e$  can exceed 60%. In the other regions the moments are affected to a lesser extent, but in general still require correcting. GS and Salem et al (2001) also describe the existence of a critical potential,  $\Phi_{\text{crit}}$ , for which the ratio  $r_N$  is zero, and no correction is required (no such critical point exists in general for the temperature or velocity). In this circumstance the energy range truncation (resulting in an under-sampled distribution) is compensated by the potential broadening caused by  $\Phi_{\text{crit}}$  such that, despite truncation and the presence of a potential, the density integration over  $f(v)$  returns the correct value.

# Chapter 5

## Calibration

### 5.1 Energy look-up tables

The *PEACE* energy range is split into 88 bins, characterised by the central energy of a bin, together with its width  $\Delta E$ . The exact energy levels of the  $i$ th level ( $E_i \pm \Delta E_i/2$ ) to be used are specific to both LEEA and HEEA and to each spacecraft. Further more, the instrument can operate in any one of three modes (LAR, MAR & HAR - *Low, Medium and High Angular Resolutions*), which also determine the exact energy to use (see Figure 5.1). To account for this we read in the telemetry value (from 0 to 89, '89' designating 'off') and look-up (in hard-coded tables in `./src/truncated_moment_corrector.c`) the correct lower or upper edge energy of the bin to apply in the calculation.

### 5.2 Overlap moments separation and sum

The overlap moments (L1L2 from LEEA and H1H2 from HEEA) are moments from the coincident energy ranges of the two sensors. Their raw format is slightly different to other data series we encounter because the data is tagged every half-spin. This means that, for LEEA say, L1 is data taken in the first half of the spin and L2 is data taken in the second half of the spin. In order to get this into a concurrent format, we must separate L1 and L2 and sum them. The result of this will be a data sequence which sums over the whole spin.

Some care must be taken at this stage. An identifier (the spin mode) indicates whether the data record comes from the first half or second half of the spin (note that these tags indicate the *start* of data, i.e. L1 is the start of the spin, and L2 is exactly halfway through the spin). With this information we can create a mask to subset the data sequence into two child sequences – one containing just the L1 data, and the other just the L2 data. We decide as a convention that all our data are to be spin-centred, that is, the time-tag will be placed half-way through a spin interval. L2 is already at this position, so we shift the L1 tags half a spin spacing (2 seconds) forward in time. Now the tags line up, we can simply add matching L1 and L2 tags together. This gives us the final L1+L2 sequence which conforms to all the other *PEACE* data we have. Note that gaps (intervals greater than 4 seconds without tags), are removed.

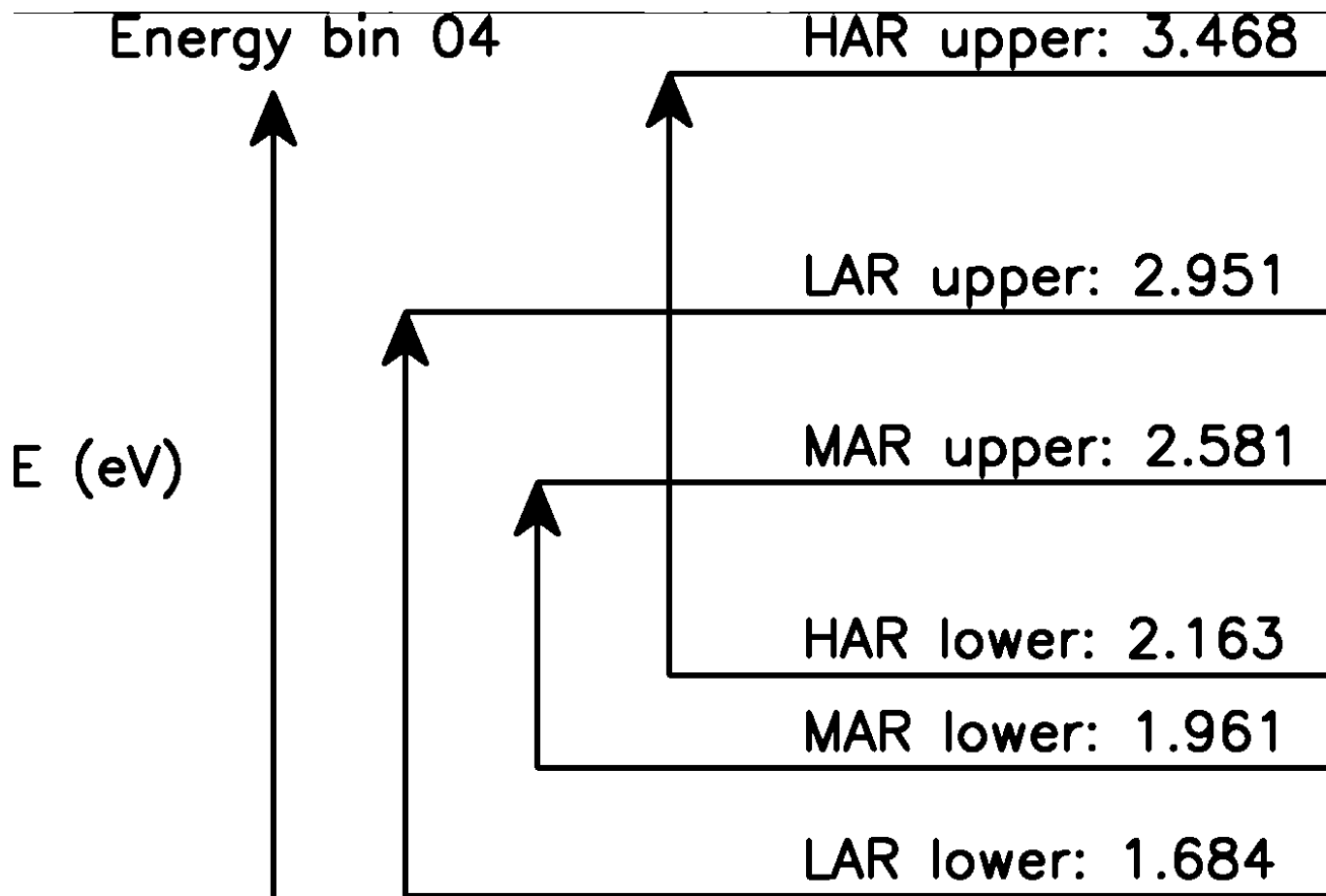


Figure 5.1: The specific energy level to be used is determined by the operating mode (LAR, MAR or HAR), the bin index and whether we wish to use the lower or upper edge of the bin. In the above example, level 04, the difference between operating modes can have an effect of several eV. At the low energy end of the integration this can have a non-negligible effect on the corrected moments.

### 5.3 Gain correction factors

All *PEACE* on-board moments data is subject to a ‘correction factor’ of 2 which is a multiplicative factor applied to all the moments as they pass through the routine. Furthermore, there is a time-dependent gain correction factor which applies to the LEEA and HEEA sensors for each spacecraft which is a further factor which varies on a time-scale of approximately 24 hours. The user supplies the location of the calibration files which must be in the following whitespace delimited format:

```
UT Start Time, UT End Time, GF Fiddle Factor, GF version no.
1930-01-01T00:00:00.000Z 2001-02-10T06:44:00.000Z 0.926227861 01_(00g01)
2001-02-10T06:44:00.000Z 2001-02-11T00:00:00.000Z 0.926227861 02_(01g01)
etc.
```

and have the names `CLN.L(H)EEA.cal`, where  $N$  is the spacecraft number 1-4. These are ex-

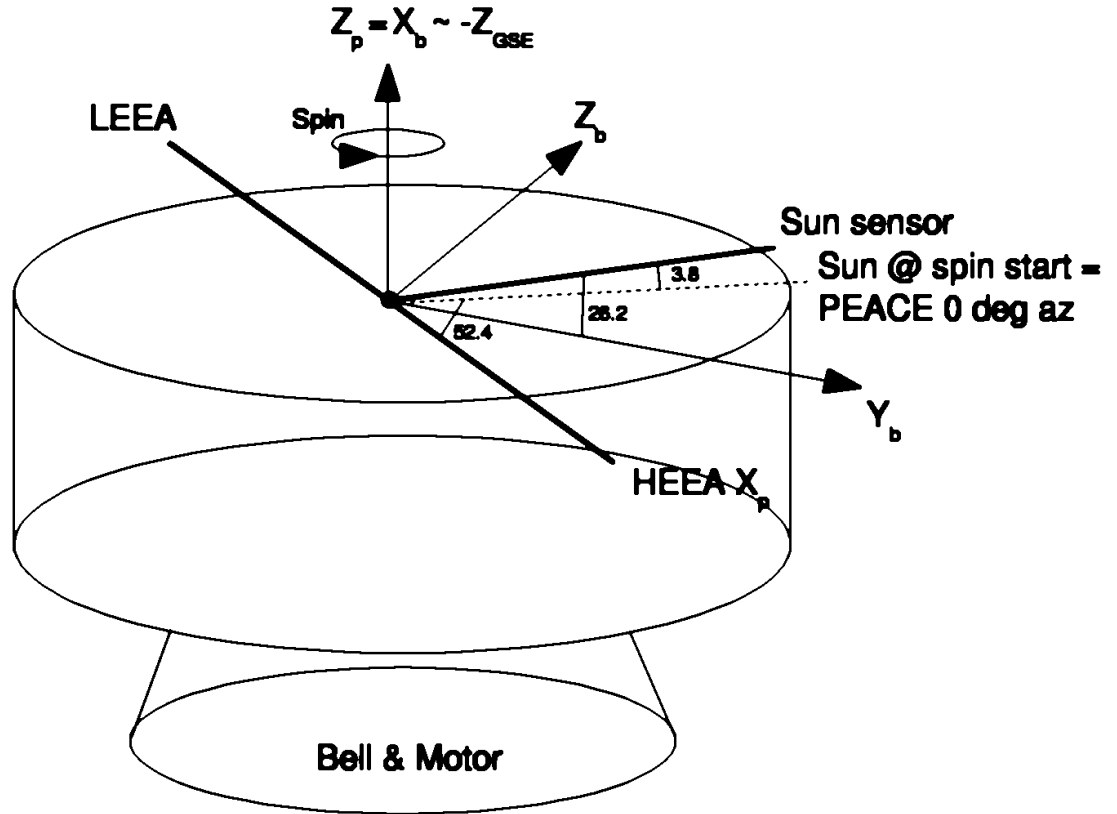


Figure 5.2: Schematic showing the principle geometry of the *PEACE* experiment.

pected to reside in the location given by the user. The correct calibration file is loaded given the input arguments.

## 5.4 Frame transformation

The moments as seen by *PEACE* are measured in a frame (hereafter the P-frame) in which the x-axis ( $X_p$ ) is aligned with the HEEA sensor head and  $Z_p$  is the spin-axis. A schematic representation of the principle *PEACE* geometry is shown in Figure 5.2. This system is different from the engineered ‘body coordinates’ (B-frame). In the B-frame the  $X_b$  is the spin axis and  $Y_b$  is 26.2 degrees antispinward of the Sun sensor. We wish to output our data in the physically informative GSE frame, so we must use attitude (AUX) data with the knowledge of the geometry of the various measurement frames to transform from the spacecraft to GSE frame.

In general, a tensor  $\mathbf{A}$  can be transformed to a new frame  $\mathbf{A}'$  by:

$$\mathbf{A}' = \mathbf{R}\mathbf{A}\mathbf{R}^T \quad (5.1)$$

where  $\mathbf{R}$  is a transformation matrix. The transformation from the raw P-frame to the GSE-frame consists of four steps. Firstly there is a 60 degree rotation about  $Z_p$  to take  $Y_p$  into  $Y_b$ , described by:

$$\begin{bmatrix} \cos(60) & -\sin(60) & 0 \\ \sin(60) & \cos(60) & 0 \\ 0 & 0 & 1 \end{bmatrix}$$

Next there is a 90 degree flip to take  $X_p$  into  $X_b$  - this is a 90 degree rotation about  $Y_b$ :

$$\begin{bmatrix} 0 & 0 & 1 \\ 0 & 1 & 0 \\ -1 & 0 & 0 \end{bmatrix}$$

Now we are in the B-frame, we must transform into the GSE frame. The inputs of latitude  $\lambda$  and longitude  $\phi$ , and knowledge of the Sun's azimuthal position at *PEACE*'s 0 degree (22.4 degrees) allow construction of two transformation matrices which deal with the spin axis orientation:

$$\begin{bmatrix} \cos(\lambda) \cos(\phi) & \beta(\sin^2(\lambda) + \cos^2(\lambda) \sin^2(\phi)) & 0 \\ \cos(\lambda) \sin(\phi) & -\beta(\cos^2(\lambda) \cos(\phi) \sin(\phi)) & \beta \sin(\lambda) \\ \sin(\lambda) & -\beta(\cos(\lambda) \sin(\lambda) \cos(\phi)) & -\beta \cos(\lambda) \sin(\phi) \end{bmatrix}$$

and the offset between  $Y_b$  and the *PEACE* 0 degree azimuthal:

$$\begin{bmatrix} 1 & 0 & 0 \\ 0 & \cos(22.4) & \sin(22.4) \\ 0 & -\sin(22.4) & \cos(22.4) \end{bmatrix}$$

The normalisation factor  $\beta$  is

$$\beta = (\sin^2(\lambda) + \cos^2(\lambda) \sin^2(\phi))^{-1/2} \quad (5.2)$$

This choice of factor accounts for the constraint that the  $t = 0$   $Y_p$  axis is 22.4 degrees spinward of  $Y_b$  and must have a positive  $X_{\text{GSE}}$  component.

Applied in the above sequence, the above matrices transform a tensor or vector from the raw P-frame into the desired GSE frame. All outputs from the solver are in GSE coordinates.

## Chapter 6

# Useful information

### 6.1 PEACE operations history key

*Note – this information is reproduced/adapted from the official PEACE operations web-site: [www.mssl.ucl.ac.uk/www.plasma/missions/cluster](http://www.mssl.ucl.ac.uk/www.plasma/missions/cluster), and was correct at the time of writing. For an up-to-date version, please visit the website*

The experiment mode can be summarised by a string, each section of which describes some aspect of the operation of PEACE:

AmB-CmD-cplrstxyf-apl-XwZ

The first two sections describe the energy coverage of HEEA and LEEA. Here HEEA is operating from level A to B, and LEEA from C to D. The next section describes how the DPU is generating moments (note that all codes have been shown in the above example, but this is only for completeness. In reality PEACE will be operating with some combination of these). The codes can be summarised as follows:

c	CORE	includes moments
p	PAD	pitch angle data
l	LER	reduced resolution low energy data
r	3DR	reduced /8 resolution data from HEEA and LEEA
s	3DR	reduced /8 resolution data from LEEA only
t	3DR	reduced /8 resolution data from HEEA only
x	3DX1	reduced by variable degree resolution 3D data, one sensor
y	3DX2	second 3DX in same spin
f	3DF	full resolution 3D data from HEEA and LEEA

Note that these operation codes appear in order of precedence. The final sections describe how the 3DX data is being calculated.

a	all azimuths (t for 2 azimuths, cartwheel slice)
p	adds together pairs of anodes (e for pairs of energy bins, n for no summing)
l	data from LEEA (h if from HEEA)
XwZ	3DX data contains a subset (levels X to Z) of the range covered by LEEA/HEEA.
nw	'no window' – there was no subsetting of energy levels

As an example, consider the operations code:

```
88m28-60m00-cplxt-apl-60w08
```

Here we can tell that HEEA was operating between levels 88 and 28 and LEEA was operating between levels 60 and 00. CORE data (c) was transmitted along with pitch angle data (p) and reduced resolution low energy data (l). There are reduced resolution 3DX moments from one sensor (x) and reduced angular resolution 3DR moments from HEEA. The 3DX moments are summed over all azimuths (a) and pairs of anodes (p) and the data comes from LEEA (l). Energy levels 00 to 08 are discarded.

## 6.2 Cluster spacecraft identifiers, nomenclature and plotting guidelines

*Note – this information is reproduced/adapted a website maintained by Mike Hapgood: [jsoc1.bnsc.rl.ac.uk/pub/cluster\\_ids.html](http://jsoc1.bnsc.rl.ac.uk/pub/cluster_ids.html), and was correct at the time of writing. For an up-to-date version, please visit the website*

### *Spacecraft identification*

ESA name	Rumba	Salsa	Samba	Tango
Launch date	2000/08/09	2000/07/16	2000/07/16	2000/08/09
ESA no.	1	2	3	4
COSPAR ID	2000-045A	2000-041B	2000-041A	2000-045B
USSPACECOM cat. no.	26463	26411	26410	26464
CSDS code	C1	C2	C3	C4
ESIC FD code	S1	S2	S3	S4
ESA flight model no.	FM5	FM6	FM7	FM8

### *Plotting guidelines*

Colour	Black	Red	Green	Magenta
Line style	Solid	Dashed	Dotted	Dash-dot-dot-dot
Symbols (line segments)	Cross	Plus	Asterisk	Star
Symbols (solid filled)	Square	Diamond	Circle	Triangle

1. ESA no. This is the spacecraft ID used in Cluster operations by ESOC and JSOC.
2. COSPAR ID (also known as the International Designation). This ID is assigned by World Data Center A for Rockets and Satellites at NASA Goddard Space Flight Center following spacecraft launch. It is the unique designator that is required for all spacecraft under international law. It takes the form YYYY-LLLI, where YYYY is the year of launch, LLL is the launch number and I is a letter that distinguishes the different items launched.
3. USSPACECOM catalogue number (also known as the NORAD catalogue number). This is the catalogue number assigned by NORAD when an object is first tracked.
4. CSDS code. This is the two-character spacecraft code used in the data products produced by the Cluster Science Data System (CSDS).
5. ESOC FD code. This is the two-character spacecraft code used in the names of orbit and event files produced by ESOC Flight Dynamics.

6. ESA Flight Model number. These are the numbers used by ESA during the construction and ground testing of the Cluster-II spacecraft. Note that this sequence follows on from that used for the construction and ground testing of the original Cluster-I spacecraft.
7. Symbols. The first set of symbols are made out of line segments, whereas the second set may be either outlines or solid-filled. Note that asterisks have 6 legs and stars have 5 points.

# Bibliography

- [1] Balogh, A., Carr, C. M., Acuña, M. H., Dunlop, M. W., Beek, T. J., Brown, P., Fornacon, K.-H., Georgescu, E., Glassmeier, K.-H., Harris, J., Musmann, G., Oddy, T. and Schwingenschuh, K., The Cluster Magnetic Field Investigation: overview of in-flight performance and initial results, *Annales Geophysicae*, 19, 1207, 2001.
- [2] Décréau, P. M. E., P. Ferreau, V. Krannosels'kikh, M. Lévêque, Ph. Martin, O. Randriamboarison, F. X. Sené, J. G. Trotignon, P. Canu, and P. B. Mogensen, Whisper, a Resonance Sounder and Wave Analyser: Performances and Perspectives for the Cluster Mission, *Space Sci. Rev.*, 79, 157, 1997.
- [3] Décréau, P. M. E., P. Ferreau, V. Krannosels'kikh, M., Le Guirriec, E, Lévêque, Ph. Martin, O. Randriamboarison, Rauch, J. L., F. X. Sené, Séran, H. C., J. G. Trotignon, P. Canu, Cornilleau, N., de Féraudy, H., Alleyne, H., Yearby, K., Mogensen, P. B., Gustafsson, G., André, M., Gurnett, D. C., Darrouzet, F., Lemaire, J., Harvey, C. C., Travnicek, P and Whisper experimenters, Early results from the Whisper instrument on Cluster: an overview, *Annales Geophysicae*, 19, 1241, 2001.
- [4] Escoubet, C. P., A. Pedersen, R. Schmidt, and P. A. Lindqvist, Density in the magnetosphere inferred from ISEE 1 spacecraft potential, *J. Geophys. Res.*, 102, 17595, 1997.
- [5] Geach, J., S. J. Schwartz, V. Génot, O. Moullard, A. Lahiff & A. N. Fazakerley, A corrector for spacecraft calculated electron moments, *Annales Geophysicae*, sub, 2004.
- [6] Génot, V. and S. J. Schwartz, Spacecraft potential effects on electron moments derived from a perfect plasma detector, *Annales Geophysicae* 22, 2073, 2004.
- [7] Grad, R. J. L., Properties of the satellite photoelectron sheath derived from photoemission laboratory measurements, *J. Geophys. Res.*, 78, 2885, 1973.
- [8] Johnstone, A. D., C. Alsop, S. Burge, P. J. Carter, A. J. Coates, A. J. Coker, A. N. Fazakerley, M. Grande, R. A. Gowen, C. Gurgiolo, B. K. Hancock, B. Narheim, A. Preece, P. H. Sheather, J. D. Winningham, and R. D. Woodliffe, Peace: a Plasma Electron and Current Experiment, *Space Sci. Rev.*, 79, 351, 1997.
- [9] Pedersen, A., Solar wind and magnetosphere plasma diagnostics by spacecraft electrostatic potential measurements, *Ann. Geophys.*, 13, 118, 1995.
- [10] Press, W. H., S. A. Teukolsky, W. T. Vetterling and B. P. Flannery, Numerical Recipes in Fortran 77: The Art of Scientific Computing, Cambridge University Press, 1992.
- [11] Salem, C. J.-M. Bosqued, D. E. Larson, A. Mangeney, M. Maksimovic, C. Perche, R. P. Lin, and J.-L. Bougeret, Determination of accurate solar wind electron parameters using particle detectors and radio wave receivers, *J. Geophys. Res.*, 106, 9, 21701, 2001.

- [12] Schmidt, R., H. Arends, A. Pedersen, F. Rudenauer, M. Fehringer, B. T. Narheim, R. Svenes, K. Kvernsveen, K. Tsuruda, T. Mukai, H. Hayakawa, and M. Nakamura, Results from active spacecraft potential control on the Geotail spacecraft, *J. Geophys. Res.*, *100*, 17253, 1995.
- [13] Song, P., X. X. Zhang, and G. Paschmann, Uncertainties in plasma measurements: effect of lower cutoff energy and spacecraft charge, *Planet. Space Sci.*, *45*, 2, 255, 1997.
- [14] Szita, S., A. N. Fazakerley, P. J. Carter, A. M. James, P. Trávníček, G. Watson, M. André, A. Eriksson, and K. Toekar, Cluster PEACE observations of electrons of spacecraft origin, *Ann. Geophys.*, *19*, 1, 2001.
- [15] Toekar, K., W. Riedler, C. P. Escoubet, M. Fehringer, R. Schmidt, R. J. L. Grard, H. Arends, F. Rüdener, W. Steiger, B. T. Narheim, K. Svenes, R. Torbert, M. André, A. Fazakerley, R. Goldstein, R. C. Olsen, A. Pedersen, E. Whipple, and H. Zhao, Active Spacecraft Potential Control for Cluster – Implementation and First Results, *Annales Geophysicae* *19*, 1289, 2001.